Active control of the tip vortex: an experimental investigation on the performance characteristics of a model turbine

To cite this article: E Anik *et al* 2014 *J. Phys.: Conf. Ser.* **524** 012098

Active control of the tip vortex: an experimental investigation on the performance characteristics of a model turbine

E Anık[1,2] , A Abdulrahim[1,2] , Y Ostovan[3,4], B Mercan[3,4], O Uzol[5,6]

[1] M.Sc., Dept. of Aerospace Engineering, METU, 06800 Ankara, Turkey
[2] Researcher, METU Center for Wind Energy, 06800 Ankara, Turkey
[3] Ph.D., Dept. of Aerospace Engineering, METU, 06800 Ankara, Turkey
[4] Scientific Project Expert, METU Center for Wind Energy, 06800 Ankara, Turkey
[5] Assoc. Prof., Dept. of Aerospace Engineering, METU, 06800 Ankara, Turkey
[6] Director, METU Center for Wind Energy, 06800 Ankara, Turkey

E-mail: ezgi.anik@metu.edu.tr

Abstract. This study is part of an on-going experimental research campaign that focuses on the active control of the tip leakage/vortex characteristics of a model horizontal axis wind turbine rotor using tip injection. This paper presents both baseline (no-injection) data as well as data with tip injection, concentrating on the effects of tip injection on power and thrust variations with the Tip Speed Ratio (TSR). The experiments are conducted by placing a specially designed 3-bladed model wind turbine rotor at the exit of a 1.7 m diameter open-jet wind tunnel. The rotor blades are non-linearly twisted and tapered with NREL S826 airfoil profile all along the span. The nacelle, hub and the blades are specifically designed to allow pressurized air to pass through and get injected from the blade tips while the rotor is rotating. Baseline results show that the general trends are as expected for a small wind turbine and the maximum power coefficient is reached at around TSR=4.5. Results with injection show that the tip injection has significant effect on the power and thrust coefficients in comparison to the baseline data, especially at TSR values higher than the max C_P TSR value. Both coefficients seem to be significantly increased due to tip injection and the max C_P TSR value also gets shifted to a slightly higher TSR value. Tip injection seems to have no significant effect for TSR values less than 3.5.

1. Introduction

The primary source of the tip vortex is the pressure difference between the upper and lower surfaces of a blade and the related flow leakage at the blade tips. When the leakage flow meets with the main stream, concentrated vortical structures get generated. These vortex structures can cause a variety of performance losses and noise problems for horizontal axis wind turbines. In addition, these vortices can cause structural and performance problems due to vortex-turbine interactions in successively arranged wind turbines in wind farms.

There are several applications of passive control methods in wind turbines in the open literature for tip leakage control such as winglets (e.g. Johansen and Sorensen (2006) [1], Elfarra et al (2014) [2], Gaunna and Johansen (2007) [3]), Mie-vanes (Shimizu et al. (1995) (2003) [4][5]) and vortex diffusers (Bai et al. (2011) [6]). Active Flow Control (AFC) is generally proposed to control the boundary layer characteristics such as transition or separation on a wind turbine. Some examples are vortex generators jets (Barrett R, Farokhi S, 1996) (Lin J C, 1999) [7][8], blowing & suction (Weaver D et al, 1996) (Bons J et al, 2002) [9][10], synthetic jets (James R D et al, 1996) (Smith B L, Glezer A, 1998) [11][12] and plasma actuators (Post M L, Corke T C, 2005) (Moreau E, 2007) (Moreau E et al, 2007) [13][14][15]. AFC using tip injection in wind turbine blades can also be applied for controlling the tip leakage/vortex characteristics. It is known that this technique increases the total lift generated from a wing/blade because of the increase in the effective span due to reduced leakage at the blade tip. Some previous implementations are fixed wings (e.g. Margaris and Gursul (2004) [16], Mercan et al (2010) [17], Ostovan (2011) [18], Bettle (2004) [19]) as well as helicopter (e.g. Duraisamy and Baeder (2004) [20], Vasilescu (2004) [21], Liu et al (2000) [22], Han and Leishan (2004) [23]) and turbomachinery blades (e.g. Mercan et al (2012) [24], Rao (2005) [25], Niu and Zang (2011) [26]).

This study is part of an on-going experimental research campaign that focuses on the active control of the tip leakage/vortex characteristics of a model horizontal axis wind turbine rotor using tip injection. In this paper we present some of the baseline measurement results obtained from a specially designed 3-bladed model wind turbine rotor as well as some of the injection cases studied. The experiments are conducted by placing this rotor at the exit of a 1.7 m diameter open-jet wind tunnel and measuring the torque and thrust characteristics without tip injection as a baseline case and with tip injection cases. The rotor blades are non-linearly twisted and tapered with NREL S826 airfoil profile all along the span. The nacelle, hub and the blades are specifically designed to allow pressurized air to pass through and get injected from the blade tips while the rotor is rotating. The setup is instrumented with a torquemeter and a load cell to allow measurements of torque and thrust. Variations of torque and thrust coefficients with Tip Speed Ratio (TSR) under different freestream conditions are obtained and presented in the following sections.

2. Experimental setup

The experiments are performed in an open jet wind tunnel facility as shown in Figure 1. The tunnel is driven by a 45 kW electric motor that runs a 1.25 m diameter axial fan. The open jet facility consists of a 4.30 m long circular diffuser with an inlet cross section diameter of 1.25 m and an exit cross section diameter of 1.70 m with a 3 deg diffusion angle. The diffuser is followed by three straight circular sections, each having a diameter of 1.70 m and a total length of 1.40 m. The total length of the tunnel is approximately 7 m. The tunnel is equipped with flow straighteners such as two turbulent screens and one honeycomb to improve the quality of the flow and ensure a uniform flow at the jet exit. The maximum velocity reached at the jet exit is around 10 m/s and the turbulence intensity levels are around 2.5%.

Figure 1. Open-jet wind tunnel facility

The model wind turbine used in the experiments is a 0.950 m diameter 3-bladed rotor with non-linearly twisted and tapered blades that have NREL S826 profile. The blade taper and twist distributions are the same as the ones used in the experiments performed at the Norwegian University of Science and Technology (NTNU) as reported in Adaramola and Krogstad (2011) [27]. The blades are manufactured using rapid prototyping techniques from ABS plastic with 0.6 mm precision. The rotational speed of the turbine is controlled by a 1.5 kW Panasonic AC servo motor. The rotor shaft is instrumented with a T20WN/5Nm torque transducer that measures the torque and rpm. The nacelle of the turbine sits on a six axes F/T transducer situated between the tower and the nacelle that measures all 6 components of forces and moments. Table 1 presents the general dimensions of the turbine and some of the turbine details are presented in Figure 2.

Table 1. Dimensions of the experimental setup

Rotor Diameter, D_{rotor} (m)	Hub Diameter, d_{hub} (m)	Hub Height, h_{hub} (m)	Wind tunnel Exit Diameter, D (m)
0.950	0.130	1.700	1.700

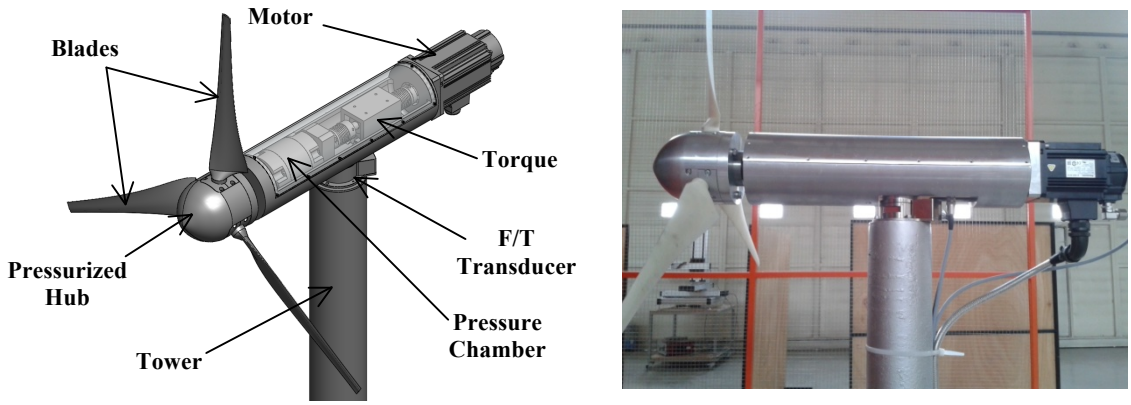

Figure 2. Model wind turbine assembly used in the experiments

The nacelle, hub and the blades are specifically designed to allow pressurized air to pass through and get injected from the tips while the rotor is rotating. The injection system consists of a pressure chamber and a hollow shaft inside the nacelle, a pressurized hub and blades with flow channels along the span embedded within the blade geometry to allow pressurized air to get injected from the tips of the blades during rotation. The pressure chamber is sealed with rotating mechanical seals, which allow rotation of the shaft passing through this chamber and also prevent air leakage. Furthermore, the connections between the shaft and the hub as well as the connections between the hub and the blades are also sealed with appropriate O-rings to prevent air leakage during air injection. The pressurized air for the injection system is supplied from outside and is connected to the pressure chamber with pneumatic quick connect interfaces as presented in Figure 3. After the pressurized air comes into the pressure chamber, it passes through the air transfer holes on the hollow shaft and is delivered to the pressurized hub. After it passes through the hub, the pressurized air is transferred through the injection channels inside the blades and finally, gets injected from the tips of the blades.

(a) (b) (c) (d)

Figure 3. (a) Pressure chamber (b) hollow shaft with air transfer holes (c) pressurized hub and (d) the rotor blade with embedded flow channel and tip injection slot.

3. Test Setup Characterization

Open-Jet Flow Characteristics

Figure 4 presents the general coordinate system definitions used in the current measurements. Figure 5 presents the results of a characterization study performed for this wind tunnel at two different selected wind tunnel motor frequencies. In order to check the boundary layer thickness and flow uniformity at the exit of the wind tunnel, instantaneous velocity measurements are performed using a single sensor hot-wire driven by a Constant Temperature Anemometer (CTA) system. The results of the characterization show that the flow is quite uniform away from the walls and around the jet centerline. The boundary layer thicknesses are below 7 mm (0.4% D) and the turbulence levels are around 2.5%.

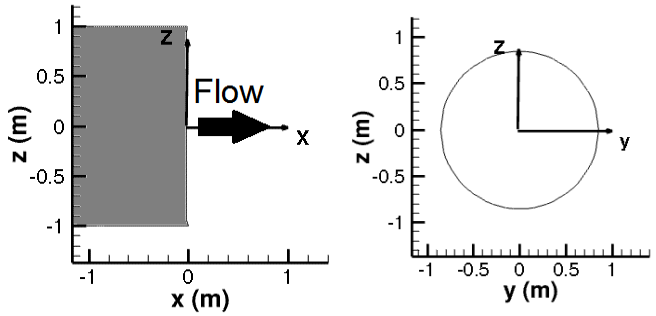

Figure 2. Coordinate system definitions used in the wind tunnel characterization and other measurements

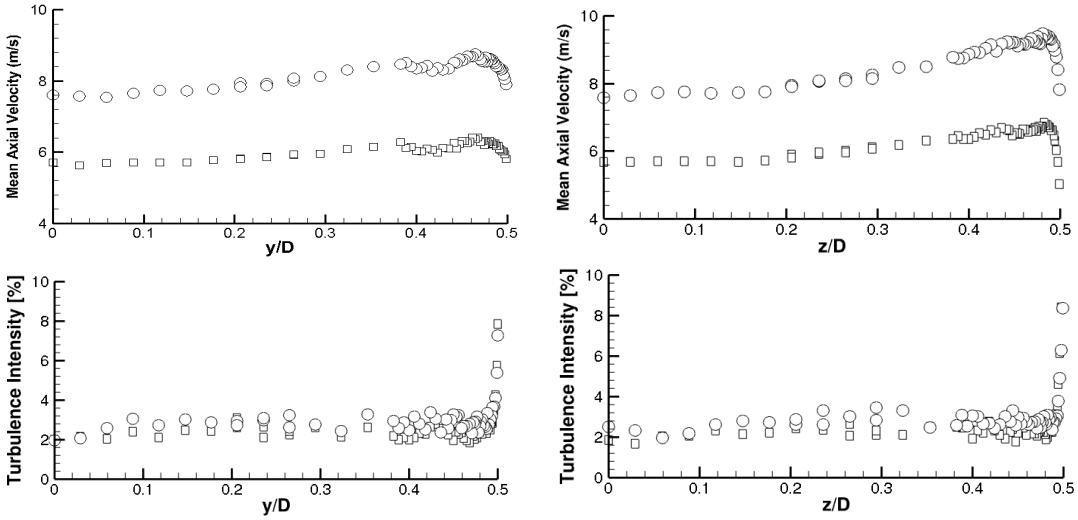

Figure 3. Mean axial velocity (top row) and turbulence intensity variations (bottom row) at the exit plane of the open-jet tunnel. Jet centerline is at (y,z)=(0,0).

Frictional torque on the shaft

Various mechanical elements that are placed on the shaft between the turbine rotor and the torque transducer such as the Pressure Chamber (PC), bearings and couplings generate a resistive frictional torque on the system. Since these elements are placed between the turbine rotor and the torque transducer, the measured torque from the transducer includes these effects and it has to be corrected appropriately to obtain the actual torque of the turbine rotor only. Normally the frictional torque generated by the bearings and couplings is small compared to the torque of the turbine rotor and is generally neglected. However, in the current test setup a significant amount of frictional torque is generated by the PC mainly due to the existence of contact rotary seals embedded inside to prevent the air leakage from the chamber. Furthermore, the frictional torque characteristics of these seals

(therefore the PC) change with rotational speed and the air pressure level inside the chamber. So for every measurement condition, i.e. rotor rpm and amount of injection level, one has to determine the actual frictional torque on the shaft generated by the PC and correct the torque measured by the torque transducer accordingly. Figure 6 shows a Free Body Diagram (FBD) of the setup showing the various torque components acting on the system.

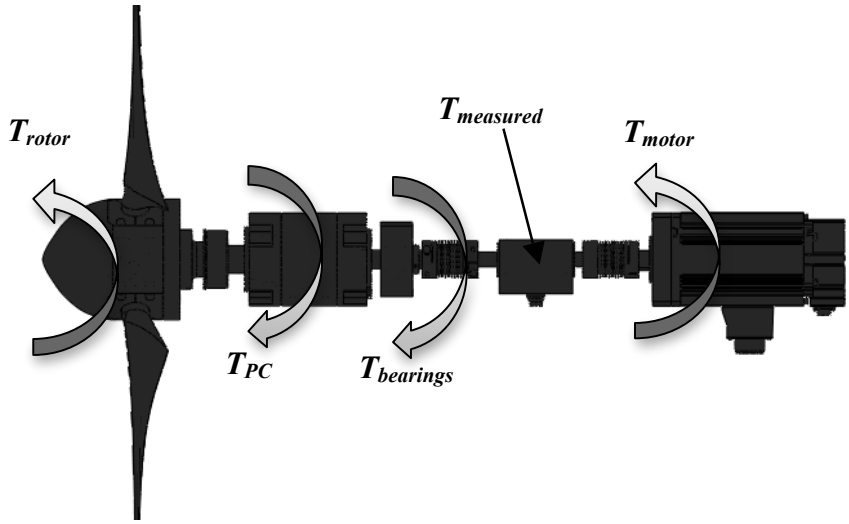

Figure 6. Free body diagram (FBD) showing various torque components acting on the shaft.

For this purpose, several measurements are performed to determine the variation of the frictional torque generated by the PC with rotational speed for injection and no-injection cases. These measurements are obtained at no wind conditions just by running the turbine rotor with the motor. Figure 7 shows the variation of the friction torque measured by the torque transducer with rotational speed when the PC is installed for no-injection and injection cases. These frictional torque data are used for correcting the measured torque to obtain the actual torque of the turbine rotor.

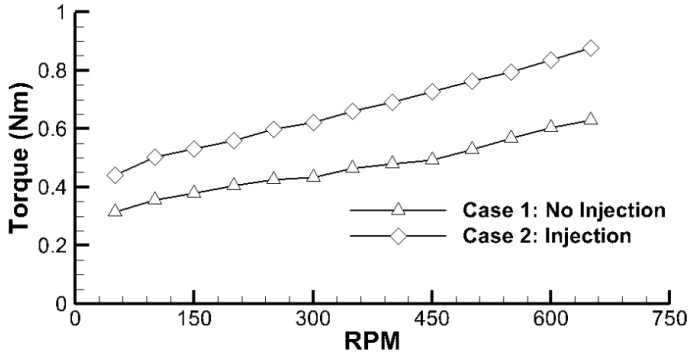

Figure 7. Frictional torque variation for no wind conditions at selected RPM

4. Results

The experiments are performed at selected wind speeds and at selected RPM values to obtain power and thrust coefficients variations with TSR for baseline (no-injection) and for the injection case measurements. The model wind turbine is placed half a rotor diameter away from the exit of the open-jet tunnel. The center of the hub and the tunnel centerline are concentric. The blades are installed at a zero pitch angle.

Baseline (No-injection) Measurements

The power and thrust coefficient variations with TSR at different wind speeds are presented in Figure 8. As it can be seen from the results, the wind turbine displays expected trends in general in terms of power and thrust variations. It's known that for small wind turbines the power coefficient depends both on the wind speed and the TSR, especially at high TSR values, unlike large turbine rotors where the power coefficient is mainly a function of TSR only (Probst O et al (2011) [29]). This characteristic is also generally attributed to the poor aerodynamic performance due to the low Reynolds number operation of small wind turbine blades (Probst O et al (2011) [29]). For this specific rotor, at every wind speed, as TSR increases C_P stays close to zero and almost constant up to about TSR=3. Then there is a sudden increase in C_P after TSR=3.5 and the rotor reaches the maximum C_P levels at around TSR=4.5. For higher TSR levels the C_P starts to decrease. For lower wind speeds and high TSR values, it can be seen that the power coefficient takes negative values. The main reason for this is that as the RPM increases the local angle of attack on the blades starts to get negative values. This causes the blades to produce negative lift and hence negative torque values generating the observed negative C_P values. The thrust coefficient variation as presented in Figure 8 shows an increasing trend with TSR as expected. Up to about TSR=3 variations for all different wind speeds collapse on to one single line. After this point deviations start to appear and as is evident at higher wind speeds the C_T value increases much faster for higher wind speeds. Note that the results get limited as TSR gets increased for high wind speeds. This was due to mainly structural integrity concerns of the current rotor blades at high RPM values.

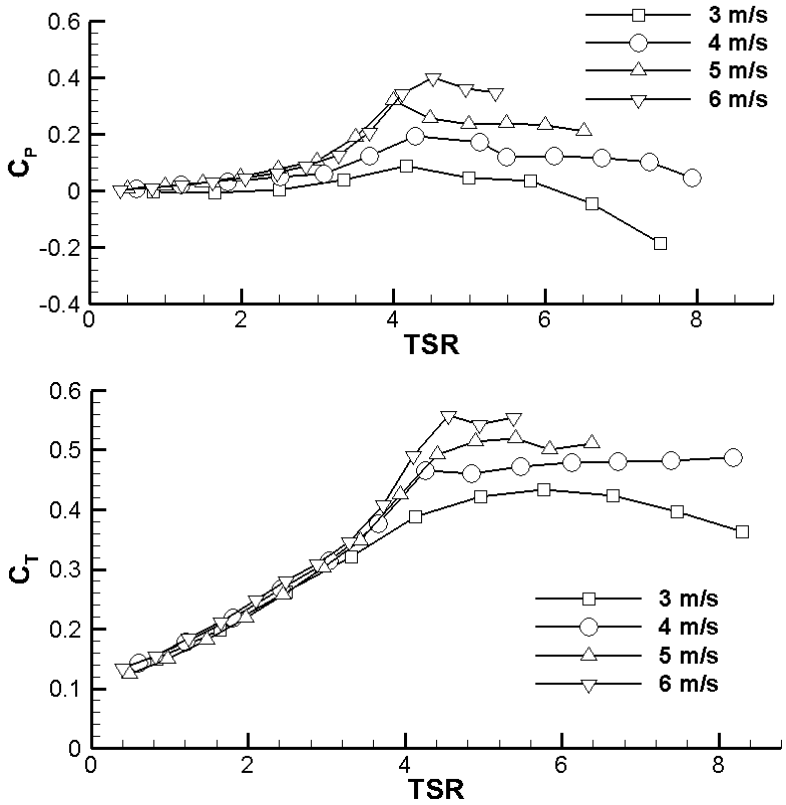

Figure 8. Measured power and thrust coefficient variations with TSR for different wind speeds

One should note that the measured thrust values do include the drag due to the hub and the nacelle because of the position of the force-moment transducer. In order to quantify this influence on the measured C_T values we measured the drag of the hub and the nacelle without the blades at selected wind speeds. Figure 9 presents the C_T distributions with TSR with and without the drag of the hub and

the nacelle. As is evident the values do get reduced slightly when hub/nacelle effect is removed. Maximum observed difference is about 13%.

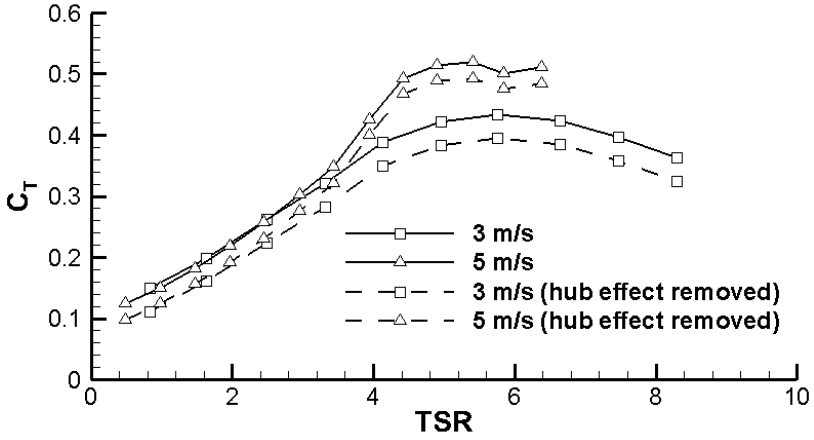

Figure 9. Measured thrust coefficient variations with TSR for selected wind speeds with and without the drag influence of the hub and the nacelle

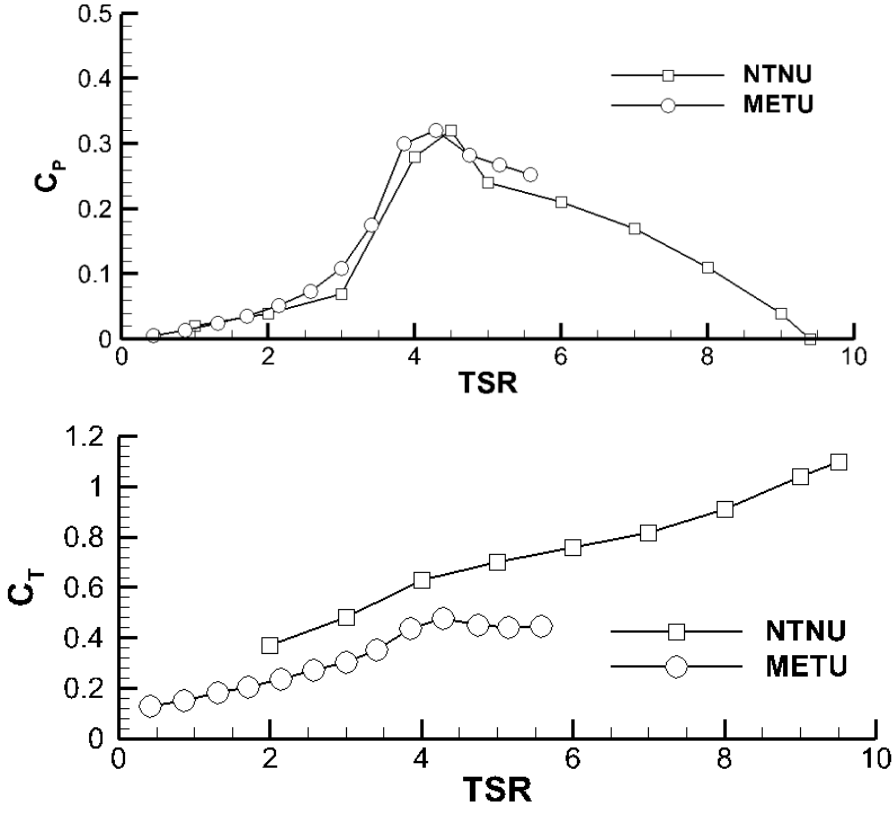

Figure 10. Comparison of measured C_p and C_T data with those obtained at Norwegian University of Science and Technology (NTNU) as presented in (Bart (2011) [28]). The data presented are obtained at 5.8 m/s wind speed.

The baseline measurement results are also compared to those obtained from the experiments conducted at the Norwegian University of Science and Technology (NTNU) using a similar turbine (Bart (2011) [28]). Both the METU and the NTNU turbines use the same NREL S826 profile as well

as the same taper and twist distributions. Due to the manufacturing restrictions imposed on the METU blades because of the existence of the internal embedded flow channels, the chords of the METU blades are reduced about 0.6 mm along the span. This corresponds to a maximum difference of 25% at the tip chord compared to the NTNU turbine. The difference gets smaller as one approaches to the root because of the increase in the chord of the blade. Also the diameter of the METU turbine is approximately 1% larger than that of the NTNU turbine. The main purpose of this comparison was to check the reliability and the confidence level of our test setup.
The C_p distribution comparison presented in Figure 10 is for a freestream wind speed of 5.8 m/s and it shows that both turbines have very similar trends in general. After TSR=3 both turbines go through a sudden increase in C_p and reaches a maximum at around TSR=4.5. The C_p values for both turbines sharply decrease after TSR=5, possibly due to laminar separation bubble on the blades caused by low Reynolds number flow (Probst O et al. (2011) [29]). This phenomenon causes severe performance losses such as increase in drag and higher uncertainties especially for Reynolds numbers lower than 100,000. Therefore for small wind turbines the power and thrust curves become a function of both TSR and wind speed for low Reynolds numbers as explained by Probst et al. (2011) [29]. The thrust coefficient variations presented in Figure 10 for both turbines also show similar trends but the METU turbine has reduced amount of thrust. The average reduction is about 35% in the thrust coefficient. The main reason behind this is the fact that the chords of the METU blades are smaller compared to those of the NTNU blades. Another reason for this reduction is due to the fact that the thrust for NTNU turbine includes the drag due to the hub, nacelle and tower respectively.

Measurements with Tip Injection
The measurements with tip injection are performed for a wind speed of 5 m/s and for a certain flow rate of injection from the blade tips. In order to determine the flow rate coming out from the blade tips, the velocity at the tip of each blade has been measured using a Pitot-Static probe while the turbine is stationary and this value is used for obtaining the outgoing mass flow rate from each blade. The average injection velocity from each blade is around a 100 m/s and the velocity variation from blade to blade is less than 5%. The ratio of the total amount of injected mass flow rate to the mass flow of air going through the rotor disk is about 0.1%.

Figure 11, shows the variations of power and thrust coefficients with TSR, with and without injection. Results show that the injection has significant effect on the power and thrust coefficients in comparison to the baseline data, especially at higher TSR values. For TSR < 3.5 the injection seems to have a minimal effect on the power coefficient data and the thrust coefficient levels seem to have slightly increased. On the other hand, for TSR>3.5 the injection starts to show substantial effects on the power and thrust coefficients. Both the power and the thrust coefficients are increased and the TSR value for maximum C_P has changed from 4 to 4.5. The maximum change in both C_P and C_T occur around TSR=4.5 and the C_P and C_T values are about 27.3% and 19.5% higher than those of the baseline no-injection case. Most probable reason for this change could be the increase in the effective span and effective aspect ratio of the blades due to the tip injection. It's known that spanwise blowing from wing tips results in induced drag reduction and lift augmentation due to an increase in effective span (Tavella D A et al (1998) [30]) (Gursul I et al (2007) [31]).

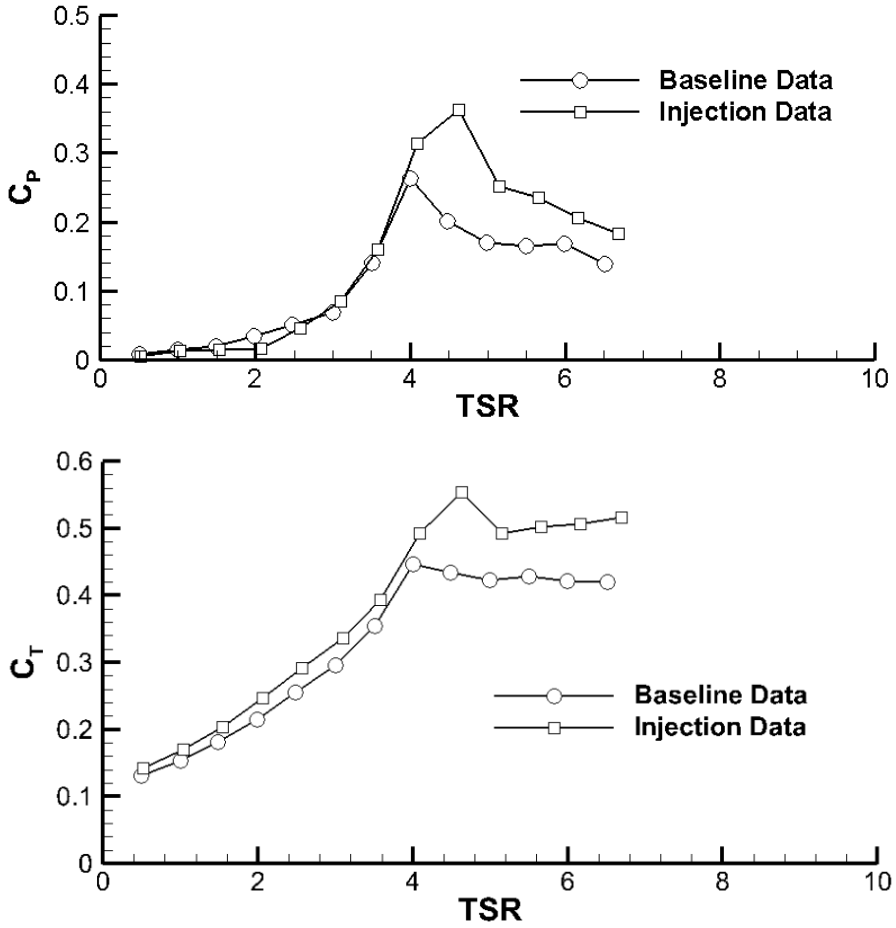

Figure 11. Measured power and thrust coefficient variations with TSR at 5 m/s wind speed, with and without tip injection.

4. Conclusions

Baseline (no-injection) as well as tip-injection performance measurements are presented for a three-bladed model horizontal axis wind turbine that is specifically designed for tip vortex control studies using tip injection. The experiments are performed in an open-jet wind tunnel and by measuring the power and thrust variations with TSR at different wind speeds for both cases. Baseline results show that the general trends are as expected for a small wind turbine and the maximum power coefficient is reached at around TSR=4.5. These baseline reference data were compared to measurement results with tip injection. Results show that the injection has significant effect on the power and thrust coefficients in comparison to the baseline data, especially at TSR values higher than the max C_P TSR value. Both coefficients seem to be significantly increased due to tip injection. Our future studies will include more data on torque and thrust measurements as well as wake flow field data with and without injection.

Acknowledgments

This study is supported by the Scientific and Technological Research Council of Turkey (*TÜBİTAK*) under the project number 112M105 as well as by METU Center for Wind Energy (*MetuWind*). Their support is greatly appreciated.

5. References

[1] Johansen J, Sørensen N N 2006 Aerodynamic investigation of Winglets on Wind Turbine Blades using CFD *Risø-R-1543(EN),* Risø National Laboratory Roskilde
[2] Elfarra, M., Sezer-Uzol, N., Akmandor, S., 2014, "NREL VI rotor blade: numerical investigation and winglet design and optimization using CFD," Wind Energy, Vol. 17, Issue 4, pp. 605-626.
[3] Gaunaa M, Johansen J 2007 Determination of the Maximum Aerodynamic Efficiency of Wind Turbine Rotors with Winglets *The Science of Making Torque from Wind, Jornal of Physics: Conference Series* 75-012006
[4] Shimizu Y, Imamura H, Matsumura S, Maeda T 1995 Power Augmentation of a Horizontal Axis Wind Turbine Using a Mie-Type Tip Vane: Velocity Distribution around the Tip of a HAWT Blade with and without a Mie-Type Tip Vane *ASME Journal Solar Energy Engineering* Vol.117 pp 297–303
[5] Shimizu Y, Ismaili E, Kamada Y, Maeda T 2003 Rotor Configuration Effect on the Performance of a HAWT with Tip-Mounted Mie-Type Vanes *ASME Journal Solar Energy Engineering* Vol. 125 pp 441–447
[6] Bai Y, Ma X, Ming X 2011 Lift Enhancement of Airfoil and Tip Flow Control for Wind Turbine *Applied Mathematics and Mechanics* Vol. 37 No. 7 pp 825-836
[7] Barrett R, Farokhi S, 1996 Subsonic Aerodynamics and Performance of a Smart Vortex Generator System *Journal of Aircraft* Vol. 33 No. 2
[8] Lin J C 1999 *Control* of Turbulent Boundary-Layer Separation using Micro-Vortex Generators *AIAA Paper* 99-3404 *30th AIAA Fluid Dynamics Conference* Norfolk VA
[9] Weaver D, McAlister K W, Tso J 1996 Suppression of Dynamic Stall by Steady and Pulsed Upper-Surface Blowing *NASA Tech. Paper* 3600 ATCOM Tech Report 95-A-005
[10] Bons J, Sondergaard R, Rivir R 2002 The Fluid Dynamics of LPT Blade Separation Control Using Pulsed Jets *ASME Journal of Turbomachinery* Vol. 124 No. 1 pp 77-85
[11] James R D, Jacobs J W, Glezer A 1996 A Round Turbulent Jet Produced by an Oscillating Diaphragm *Phys. Fluids* 8:2484
[12] Smith B L, Glezer A 1998 The Formation and Evolution of Synthetic *Jets Physics of Fluids* Vol. 10 no. 9 pp 2281-2297
[13] Post M L, Corke T C 2005 Overview of Plasma Flow Control: Concepts, Optimization and Applications *AIAA Paper* 2005-0563
[14] Moreau E 2007 Airflow Control by Non Thermal Plasma Actuators *Journal of Phys. D* 40: 605-636
[15] Moreau E, Benard N, Jolibois M, Touchard G 2007 Airflow Control by Plasma Actuators: Last Significant Results at the University of Poitiers *2nd European Conference for Aerospace Sciences*
[16] Margaris P, Gursul I 2004 Effect of Steady Blowing on Wing Tip Flowfield *AIAA* 2004-2619. *2nd Flow Control Conference* Portland Oregon USA.
[17] Mercan, B., Ostovan, Y., Doğan, E., Uzol, O., 2010, "Effect of Chordwise Modulated Waveform Tip Injection on the Characteristics of the Tip Vortex," 40th Fluid Dynamics Conference and Exhibit, Chicago, Illinois, June 28-1.
[18] Ostovan Y 2011 Experimental Investigation of Waveform Tip Injection on the Characteristics of the Tip Vortex *M.Sc. Thesis* Middle East Technical University
[19] Bettle J R 2004 Experimental Study of a Wing Tip Vortex with Tip Blowing *M.Sc. Thesis* The University of New Brunswick Canada
[20] Duraisamy K, Baeder J D 2004 Control of Helicopter Rotor Tip Vortex Structure Using Blowing Devices *60th Annual Forum Proceedings, American Helicopter Society* Vol. 2 pp 1952-1967
[21] Vasilescu R 2004 Helicopter Blade Tip Vortex Modifications in Hover Using Piezoelectrically Mounted Blowing *PhD Thesis* Georgia Institute of Technology
[22] Liu Z, Sankar L N, Hassan A A 2000 Alternation of the Tip Vortex Structure of a Hovering Rotor Using Oscillatory Jet Excitation *AIAA Paper* 99-0906

[23] Han Y O, Leishan J G 2004 Investigation of Helicopter Rotor-Blade-Tip-Vortex Alleviation Using a Slotted Tip *AIAA Journal* Vol. 42 No. 3 pp 524-535
[24] Mercan B, Doğan E, Ostovan Y, Uzol O 2012 Experimental Investigation of the Effects of Waveform Tip Injection in a Low Pressure Turbine Cascade *ASME Turbo Expo* 2012 Copenhagen Denmark
[25] Rao N M 2005 Desensitization of over Tip Leakage in an Axial Turbine Rotor by Tip Surface Coolant Injection *PhD Thesis* Pennsylvania State University
[26] Niu M, Zang S 2011 Experimental and Numerical Investigations of Tip Injection Clearance Flow in an Axial Turbine Cascade *Journal of Experimental Thermal and Fluid Science* 35 1214-1222
[27] Adaramola, Krogstad 2011 Experimental investigation of wake effects on wind turbine performance *Renewable Energy* Vol. 36 Issue 8 pp. 2078-2086
[28] Bartl J 2011 Wake Measurements behind an Array of Two Model Wind Turbines *M.Sc. Thesis* Norwegian University of Science and Technology
[29] Probst O, Martínez J, Elizondo J, Monroy O 2011 Small Wind Turbine Technology Wind Turbines Dr. Ibrahim Al-Bahadly (Ed.) ISBN: 978-953-307-221-0 InTech DOI: 10.5772/15861 available from http://www.intechopen.com/books/wind-turbines/small-wind-turbine technology
[30] Tavella D A, Wood N J, Lee C S, Roberts L 1998 Lift Modulation with Lateral Wing- Tip Blowing *Journal of Aircraft* Vol. 25 No. 4 pp 311-316
[31] Gursul I, Vardaki E, Margaris P, Wang Z 2007 Control of Wing Vortices Active Flow Control *Notes on Numerical Fluid Mechanics and Multidisciplinary Design* pp.137-151 Springer-Verlag Berlin